Highly Efficient and Thermally Stable Polymer Solar Cells with Dihydronaphthyl-Based [70]Fullerene Bisadduct Derivative as the Acceptor

ARTICLE *in* ADVANCED FUNCTIONAL MATERIALS · MAY 2012

Impact Factor: 11.81 · DOI: 10.1002/adfm.201102771

9 AUTHORS, INCLUDING:

Zhan'ao Tan
North China Electric Power University
88 PUBLICATIONS **3,456** CITATIONS
SEE PROFILE

Taishan Wang
Chinese Academy of Sciences
62 PUBLICATIONS **1,248** CITATIONS
SEE PROFILE

Li Jiang
Chinese Academy of Sciences
96 PUBLICATIONS **1,279** CITATIONS
SEE PROFILE

Chunying Shu
Chinese Academy of Sciences
98 PUBLICATIONS **1,948** CITATIONS
SEE PROFILE

Highly Efficient and Thermally Stable Polymer Solar Cells with Dihydronaphthyl-Based [70]Fullerene Bisadduct Derivative as the Acceptor

Xiangyue Meng, Wenqing Zhang, Zhan'ao Tan, Yongfang Li, Yihan Ma, Taishan Wang, Li Jiang, Chunying Shu, and Chunru Wang**

The efficiency of polymer solar cells (PSCs) can be essentially enhanced by improving the performance of electron-acceptor materials, including by increasing the lowest unoccupied molecular orbital (LUMO) level, improving the optical absorption, and tuning the material solubility. Here, a new soluble C_{70} derivative, dihydronaphthyl-based C_{70} bisadduct ($NC_{70}BA$), is synthesized and explored as acceptor in PSCs. The $NC_{70}BA$ has high LUMO energy level that is 0.2 eV higher than [6,6]-phenyl-C_{61}-butyric acid methyl ester (PCBM), and displays broad light absorption in the visible region. Consequently, the PSC based on the blend of poly(3-hexylthiophene) (P3HT) and $NC_{70}BA$ shows a high open-circuit voltage (V_{oc} = 0.83 V) and a high power conversion efficiency (PCE = 5.95%), which are much better than those of the P3HT:PCBM-based device (V_{oc} = 0.60 V; PCE = 3.74%). Moreover, the amorphous nature of $NC_{70}BA$ effectively suppresses the thermally driven crystallization, leading to high thermal stability of the P3HT:$NC_{70}BA$-based solar cell devices. It is observed that the P3HT:$NC_{70}BA$-based device retains 80% of its original PCE value against thermal heating at 150 °C over 20 h. The results unambiguously indicate that the $NC_{70}BA$ is a promising acceptor material for practical PSCs.

1. Introduction

Polymer solar cells (PSCs) have drawn broad attention because of their advantages of low cost, light weight, and flexibility.[1] The most efficient architecture of PSCs reported so far is the bulk heterojunction (BHJ) structure of a blend of a conjugated polymer donor and a soluble fullerene acceptor with an interpenetrating network as the photoactive layer.[2] In this architecture, poly(3-hexylthiophene) (P3HT) and [6,6]-phenyl-C_{61}-butyric acid methyl ester (PCBM) are the most representative conjugated polymer donor and acceptor materials, respectively. The power conversion efficiency (PCE) of PSCs based on P3HT:PCBM has reached over 4%.[3] However, further improving the PCE of P3HT:PCBM-based PSCs is difficult for the following reasons: i) the absorption of P3HT mismatches with solar illumination; ii) the acceptor material [60]PCBM has weak absorption in the visible region; and, iii) the typical open circuit voltage of P3HT:PCBM-based PSCs is only 0.6 V, due to the higher-lying highest occupied molecular orbital (HOMO) of P3HT and the lower-lying lowest unoccupied molecular orbital (LUMO) of PCBM. In order to improve the PCE of PSCs, over the last decades great efforts have been devoted to exploring both new conjugated polymer donor[4] and new fullerene derivative acceptor materials.[5] For conjugated polymer donor materials, the main research interests are in synthesizing some materials with broad light absorption, low bandgap, high hole mobility, and appropriate electronic energy levels.[6] For acceptor materials, however, the best candidates are expected to have properties such as strong absorption in the visible region in order to absorb more solar energy,[7] good solubility in order to get better dispersion while fabricating solar cell devices,[8] and a high level of the LUMO energy to enhance the open circuit voltage (V_{oc}).[9]

In fact, the V_{oc} of PSCs is considered to be one of the most important factors in evaluating active materials; it is proportionally determined by the difference between the LUMO energy level of the acceptor and the HOMO energy level of the donor.[10] Recently, a series of high V_{oc} P3HT-based PSCs have been obtained using fullerene derivatives with higher LUMO level as

X. Y. Meng, Y. H. Ma, T. S. Wang, L. Jiang, Prof. C. Y. Shu, Prof. C. R. Wang
Key Laboratory of Molecular Nanostructure and Nanotechnology
Beijing National Laboratory for Molecular Sciences
Institute of Chemistry
Chinese Academy of Sciences
Beijing 100190, China
E-mail: crwang@iccas.ac.cn
X. Y. Meng, Y. H. Ma
Graduate University of Chinese Academy of Sciences
Beijing 100049, China
W. Q. Zhang, Prof. Z. A. Tan
State Key Laboratory of Alternate Electrical Power System with Renewable Energy Sources
The New and Renewable Energy of Beijing Key Laboratory
North China Electric Power University
Beijing 102206, China
E-mail: tanzhanao@ncepu.edu.cn
Prof. Y. F. Li
Key Laboratory of Organic Solids
Institute of Chemistry
Chinese Academy of Sciences
Beijing 100190, China

DOI: 10.1002/adfm.201102771

acceptors. For example, Lenes et al.[11] synthesized [60]PCBM bisadduct (bisPCBM) with a LUMO level which is 0.1 eV higher than PCBM, and the corresponding V_{oc} and PCE of the P3HT-based PSC are respectively 0.73 V and 4.5%. In comparison, the P3HT:PCBM-based solar cell has V_{oc} and PCE at 0.58 V and 3.4% under same conditions. Ross et al.[12] prepared an endohedral fullerene $Lu_3N@C_{80}$ –PCBH which also possesses a higher LUMO level than PCBM, and the PSC fabricated by P3HT:$Lu_3N@C_{80}$ –PCBH showed both high V_{oc} (0.81 V) and high PCE (4.2%) in comparison with that based on P3HT:PCBM (V_{oc} = 0.63 V and PCE = 3.4%). Other than the PCBM family of fullerene derivatives, some new bisadduct fullerene derivatives[13] were also explored to increase the LUMO energy level of fullerene acceptors and enhance the photovoltaic performance of the PSCs. Especially, Li et al.[14] recently prepared the indene-C_{60} bisadduct (ICBA), whose LUMO energy level is 0.17 eV higher than PCBM. The optimized PSCs based on P3HT:ICBA have a high V_{oc} (0.84 V) with a PCE as high as 6.48%.[15] Very recently, we reported a new dihydronaphthyl-based [60]fullerene bisadduct derivative ($NC_{60}BA$).[16] Not only does the PSC based on this material (P3HT:$NC_{60}BA$) have high V_{oc} at 0.82 V as well as high PCE at 5.37%, but also the preparation of this material is high yield at mild temperature. Therefore, this family of fullerene derivatives has potential to be applied in practice PSCs in the future.

Since it is well known that [70]PCBM-based PSCs exhibit higher PCE than [60]PCBM under the same conditions,[17] herein we explored the synthesis of C_{70} dihydronaphthyl-based bisadduct ($NC_{70}BA$) as well as the photovoltaic performance in P3HT-based PSCs. The LUMO energy level of $NC_{70}BA$ is 0.2 eV higher than that of PCBM. As expected, $NC_{70}BA$ displays improved light absorption in the visible region. Consequently, when $NC_{70}BA$ is used in the photovoltaic cell instead of $NC_{60}BA$, 8% higher current densities are obtained. The PCE of P3HT:$NC_{70}BA$-based PSCs reached 5.95%. In addition, the P3HT:$NC_{70}BA$-based devices exhibited enhanced thermal stability compared to PCBM-based PSCs.

2. Results and Discussion

2.1. Synthesis of $NC_{70}BA$

The Diels-Alder reaction of fullerene with ortho-quinodimethane provides a powerful method for fullerene functionalization.[18] The synthetic route of $NC_{70}BA$ is shown in **Scheme 1**. First, the sultine was prepared from 1,2-bis(bromomethyl)benzene by reaction with sodium hydroxymethanesulfinate ("rongalite") in anhydrous *N,N*-dimethylformamide (DMF) with a catalytic amount of tetrabutylammonium bromide (TBAB) at 0 °C. Under these conditions,[19] polymerization of the *o*-quinodimethane is avoided. The sultine then generated *o*-quinodimethanes by extrusion of SO_2, which acted as the dienophile to react with fullerene readily. The raw product was purified by silica gel column chromatography and HPLC in succession. Figure S1 shows the HPLC curve of the reaction

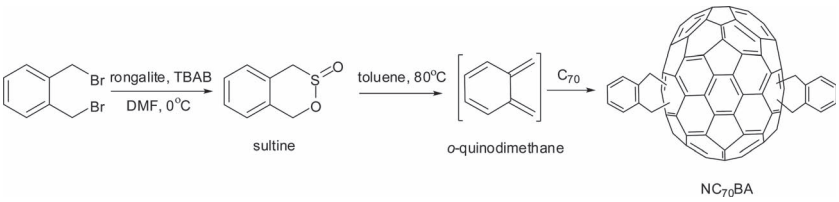

Scheme 1. Structure and synthetic route of $NC_{70}BA$.

mixture with a Buckyprep column using toluene as the eluent (see the Supporting Information).

$NC_{70}BA$ possesses excellent solubility in common organic solvents such as THF, chloroform, toluene, and *o*-dichlorobenzene. The molecular structure of $NC_{70}BA$ was confirmed by MALDI-TOF MS. It should be mentioned that the obtained $NC_{70}BA$ was a mixture of isomers, as confirmed by ^1H and ^{13}C NMR spectra; this mixture was used directly to fabricate the photovoltaic devices without further separation.

2.2. Absorption Spectra of $NC_{70}BA$

The UV-Vis absorption spectrum of $NC_{70}BA$ in THF is shown in **Figure 1**. For comparison, the absorption spectra of PCBM and $NC_{60}BA$ are also shown in the same figure. All these fullerene derivatives display strong UV absorption from 200 to 400 nm. However, the absorbance of $NC_{70}BA$ is dramatically enhanced compared to those of PCBM and $NC_{60}BA$ in the visible region from 400 to 800 nm (see the inset of Figure 1). The relatively lower absorption of C_{60} derivatives can be attributed to a high degree of symmetry, leading to the lowest-energy transitions being formally dipole forbidden. When the C_{60} moiety in $NC_{60}BA$ is replaced by a less symmetrical fullerene C_{70}, these transitions will become allowed and a dramatic increase in light absorption is expected. Obviously, $NC_{70}BA$ as acceptor material to fabricate PSCs would be able to absorb more solar energy and contribute to an improved performance.

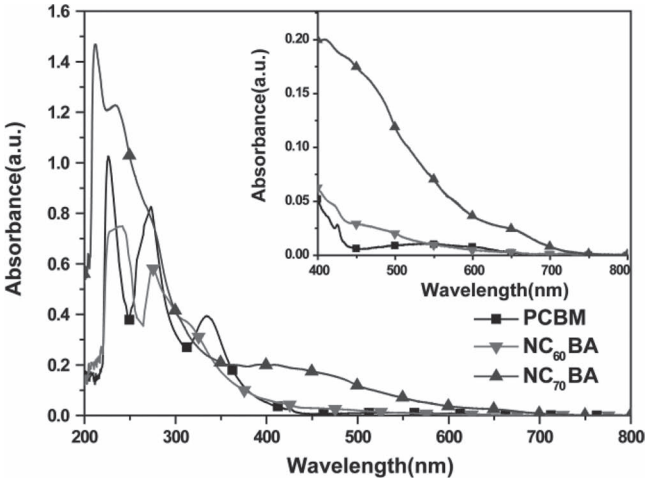

Figure 1. Absorption spectra of PCBM, $NC_{60}BA$, and $NC_{70}BA$ in THF solutions (10^{-5} mol L^{-1}). Inset: enlarged absorption spectra in the visible region from 400 to 800 nm.

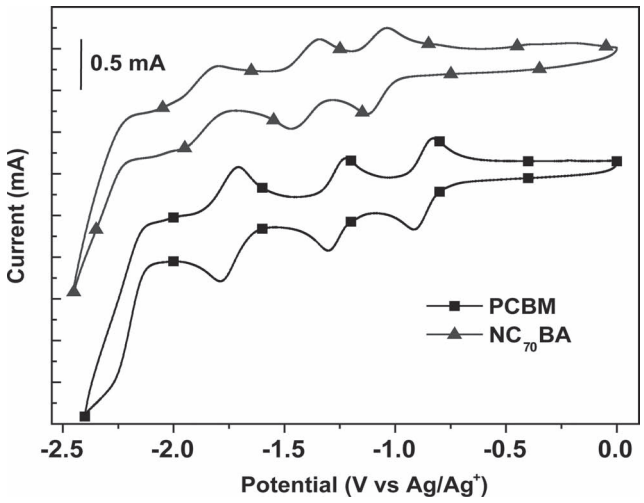

Figure2. Cyclic voltammograms of PCBM and $NC_{70}BA$ in *o*-dichlorobenzene:-acetonitrile (5:1 v/v) with 0.1 M NBu_4PF_6 at 100 mV s^{-1}.

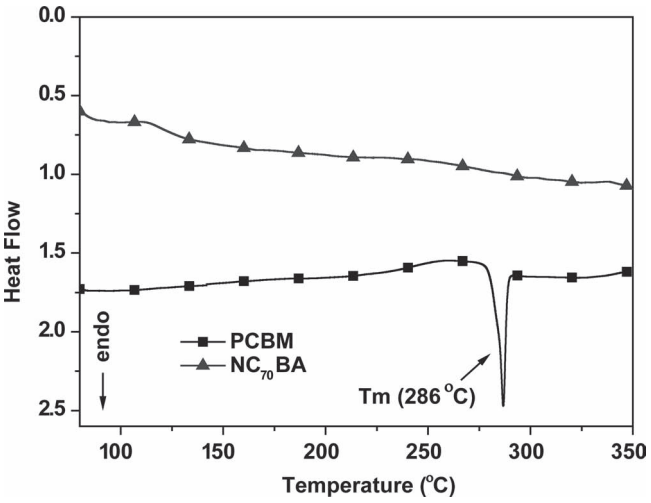

Figure 3. Differential scanning calorimetry (DSC) measurements of PCBM and $NC_{70}BA$ with a heating rate of 10 °C min^{-1}.

2.3. Electrochemical Properties of $NC_{70}BA$

The electrochemical properties of $NC_{70}BA$ were studied by cyclic voltammetry. **Figure 2** shows the cyclic voltammogram of $NC_{70}BA$ as well as that of PCBM for comparison. Both $NC_{70}BA$ and PCBM exhibit three quasi-reversible reduction waves in the negative potential range from 0 to –2.5 V vs. Ag/Ag^+. **Table 1** lists the half-wave potentials (defined as $E = 0.5[E_{p,c} + E_{p,a}]$, where $E_{p,c}$ is the cathodic peak potential and $E_{p,a}$ the corresponding anodic peak potential) of the reduction processes of the fullerene derivatives $NC_{70}BA$ and PCBM for comparison. It can be observed clearly that the first (E_1), second (E_2) and third (E_3) reduction potentials of $NC_{70}BA$ all shifted negatively compared to those of PCBM, and the onset reduction potential of $NC_{70}BA$ (–0.99 V) is also negatively shifted comparing to PCBM (–0.79 V). Moreover, the LUMO energy levels of the fullerene derivatives can be calculated from the onset reduction potentials (E_{red}^{on}) according to the following equation,[20]

$$E_{LUMO} = -\,e(E_{red}^{on} + 4.71)[eV]$$

where the unit of E_{red}^{on} is V vs. Ag/Ag^+. With this equation, the LUMO energy levels of $NC_{70}BA$ and PCBM are calculated as –3.72 and –3.92 eV, respectively. Obviously, the LUMO level of $NC_{70}BA$ is increased by ca. 0.2 eV in comparison with that of PCBM. Undoubtedly, the higher LUMO energy level of $NC_{70}BA$ is desirable for its application as an acceptor in P3HT-based PSCs because it is expected to increase the open-circuit voltage of the devices.

Table 1. Electrochemical properties of $NC_{70}BA$ and PCBM.

Acceptors	E_1 [V]	E_2 [V]	E_3 [V]	E_{red}^{on} [V]	LUMO [eV]
PCBM	–0.87	–1.26	–1.75	–0.79	–3.92
$NC_{70}BA$	–1.08	–1.41	–1.96	–0.99	–3.72

2.4. Thermal Properties of $NC_{70}BA$

The thermal properties of the fullerene acceptor are closely related to the lifetime of practical PSC devices. **Figure 3** shows differential scanning calorimetry (DSC) measurements of $NC_{70}BA$ and PCBM. In contrast to the PCBM with a crystallization peak at ca. 286 °C, no crystallization transition was observed for $NC_{70}BA$ over the whole temperature range, indicating that $NC_{70}BA$ is essentially an amorphous material. Thus it is expected that this material is able to overcome thermally driven crystallization and achieve high thermal stability in the as-fabricated PSCs.[21] Furthermore, thermal gravimetric analysis of $NC_{70}BA$ was also performed (**Figure 4**); the decomposition temperature (T_d) of $NC_{70}BA$ is as high as 415 °C, confirming the high thermal stability of this compound.

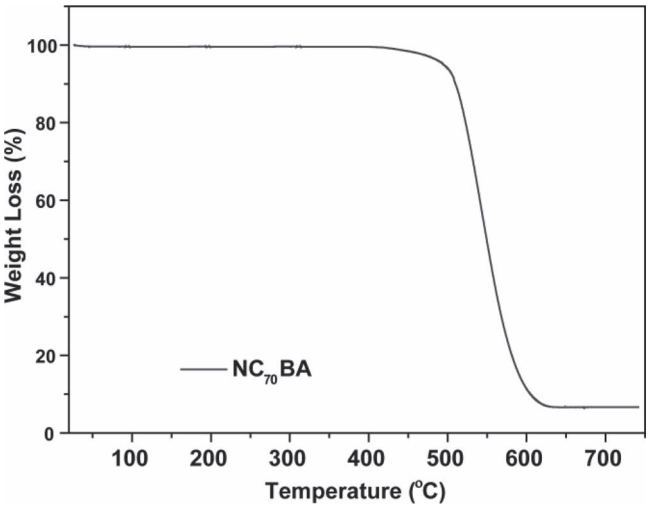

Figure 4. Thermogravimetric analysis (TGA) of $NC_{70}BA$ with a heating rate of 20 °C min^{-1}.

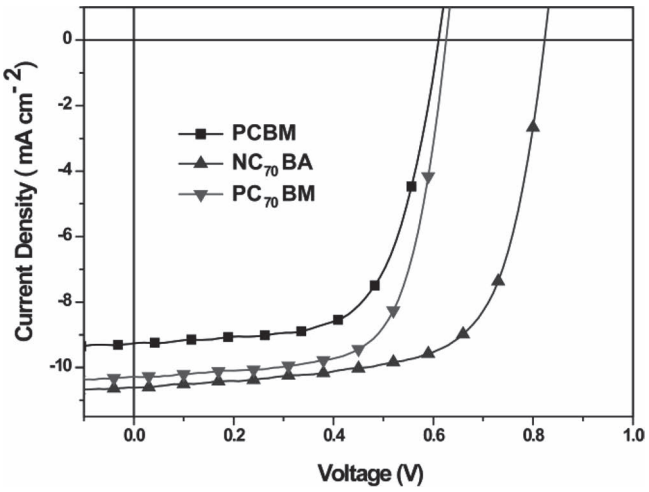

Figure 5. Current density–voltage curves of PSCs based on P3HT:$NC_{70}BA$, P3HT:PCBM, and P3HT:$PC_{70}BM$ blends.

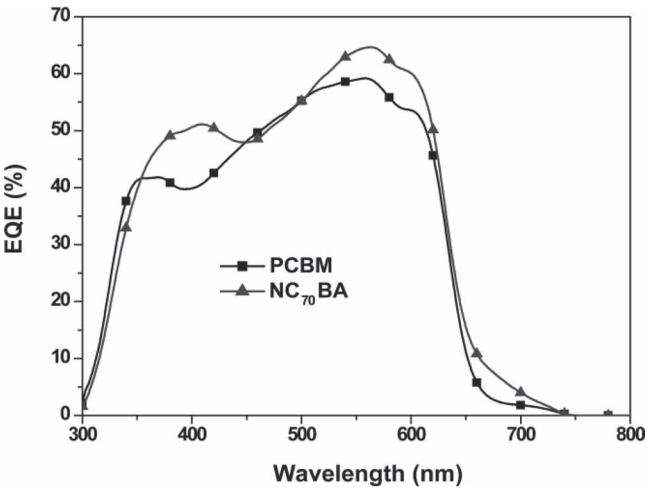

Figure 6. External quantum efficiency (EQE) of the PSCs based on P3HT:$NC_{70}BA$ and P3HT:PCBM blends.

2.5. Photovoltaic Properties of $NC_{70}BA$

To investigate the photovoltaic properties of $NC_{70}BA$, BHJ solar cells based on the ITO/PEDOT:PSS/P3HT:acceptor/Ca/Al configuration were fabricated and characterized under simulated AM 1.5 G illumination (100 mW cm^{-2}); two other devices using PCBM and $PC_{70}BM$ as acceptor materials were also fabricated as comparison. **Figure 5** shows the current density–voltage curves of the three devices; the V_{oc}, short-circuit currents (J_{sc}), fill factors (FF), and power conversion efficiencies (PCE) are listed in **Table 2**. The two control devices (P3HT:PCBM and P3HT:$PC_{70}BM$) showed PCEs of 3.74% (V_{oc} = 0.60 V, J_{sc} = 9.42 mA cm^{-2}, and FF = 0.66) and 4.32% (V_{oc} = 0.61 V, J_{sc} = 10.45 mA cm^{-2}, and FF = 0.68), respectively. In comparison, a high PCE of 5.95% was achieved from the $NC_{70}BA$-based BHJ solar cell (V_{oc} = 0.83 V, J_{sc} = 10.71 mA cm^{-2}, and FF = 0.67), which is also higher than that of the P3HT:$NC_{60}BA$ BHJ solar cell in our previous study[16] (PCE = 5.37%, V_{oc} = 0.82 V, J_{sc} = 9.88 mA cm^{-2}, and FF = 0.67). The higher V_{oc} resulting from the higher LUMO energy level of $NC_{70}BA$ was the premise for $NC_{70}BA$-based devices achieving better performance. Moreover, a value of J_{sc} = 10.71 mA cm^{-2} was observed for $NC_{70}BA$-based devices, which is enhanced by ca. 8% compared to the $NC_{60}BA$-based device, ascribed to the increased and broad absorption of $NC_{70}BA$. $NC_{70}BA$ effectively increases the V_{oc} and the J_{sc} of the device, so finally the P3HT:$NC_{70}BA$-based device shows excellent photovoltaic performance.

Table 2. Photovoltaic performance of P3HT-based PSCs with different acceptors.

Acceptor	V_{oc} [V]	J_{sc} [mA cm^{-2}]	FF	PCE [%]
PCBM	0.60	9.42	0.66	3.74
$PC_{70}BM$	0.61	10.45	0.68	4.32
$NC_{60}BA$[a)]	0.82	9.88	0.67	5.37
$NC_{70}BA$	0.83	10.71	0.67	5.95

[a)]See ref. [16].

The external quantum efficiencies (EQE) of PSCs based on P3HT:$NC_{70}BA$ and P3HT:PCBM are shown in **Figure 6**. High EQE values were observed in both NC_{70} BA- and PCBM-based devices, which suggests that the photon–electron conversion processes are rather efficient. The calculated short current density of P3HT:$NC_{70}BA$ and P3HT:PCBM devices from EQE curves were 10.18 and 8.95 mA cm^{-2}, respectively, which confirms the high J_{sc} values of the devices. The higher EQE of the $NC_{70}BA$-based PSC than PCBM-based PSC could be ascribed to the contribution of the absorption of the C_{70} derivative acceptor. The EQE result indicates that $NC_{70}BA$ is beneficial to the solar light harvest and photocurrent conversion of the P3HT-based PSCs.

2.6. Thermal Stability of the PSC Devices

When the solar cells are used outdoors under strong sunlight, the devices must withstand high temperatures. It is well known that the poor thermal stability of P3HT:PCBM solar cells results in a gradual decrease of the efficiency upon heating. To investigate the thermal stability of $NC_{70}BA$-based devices, PSCs based on P3HT:$NC_{70}BA$ and P3HT:PCBM were isothermally heated at 150 °C for 5, 10, and 20 h prior to the deposition of top electrode. A previous study had already demonstrated that amorphous fullerene materials would lead to high thermal stability of PSCs,[21] so the amorphous $NC_{70}BA$ material was favorably expected to achieve thermally stable PSCs. **Figure 7** shows the current density–voltage curves of the solar cells; the corresponding photovoltaic parameters of these devices are shown in **Table 3**. The results indeed revealed a high thermal stability of the P3HT:$NC_{70}BA$-based devices, whose PCE only slightly decreased from 5.88% to 4.89% after heating at 150 °C for 20 h. In contrast, the PCE of the P3HT:PCBM-based device significantly decreased from 3.82% to 1.75% over 20 h of heating.

To further investigate the high thermal stability of $NC_{70}BA$-based devices, in situ morphological characterization of P3HT:$NC_{70}BA$ and P3HT:PCBM blends was performed using an optical microscope. As shown in **Figure 8**, no obvious phase segregation was

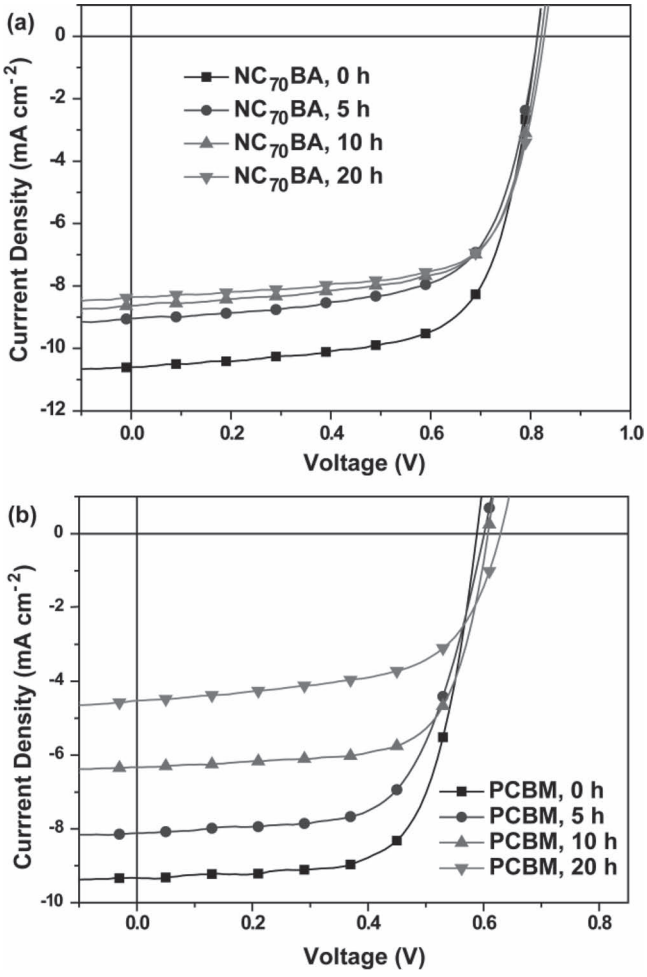

Figure 7. Current density–voltage curves of the PSCs based on: a) P3HT:$NC_{70}BA$ and b) P3HT:PCBM blends before and after isothermal heating at 150 °C for 5, 10, and 20 h, respectively.

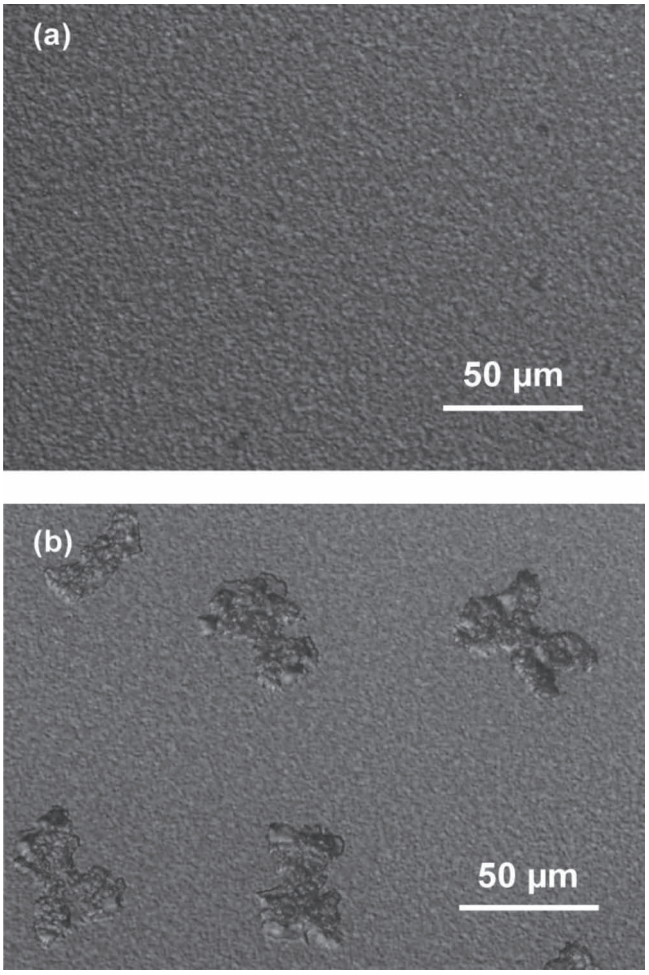

Figure 8. Optical microscopy images of: a) P3HT:$NC_{70}BA$ and b) P3HT:PCBM blends after heating at 150 °C for 20 h.

observed for the P3HT:$NC_{70}BA$ blend after thermal annealing for 20 h; in contrast, obvious PCBM aggregates appeared for the P3HT:PCBM blend after 20 h under same conditions, indicating that thermally driven crystallization for PCBM did exist, finally leading to the D-A (donor-acceptor) phase separation.

Table 3. Values of photovoltaic parameters of the P3HT-based devices as a function of heating time at 150 °C.

Acceptor	Heating time [h]	V_{oc} [V]	J_{sc} [mA cm^{-2}]	FF	PCE [%]
PCBM	0	0.59	9.30	0.70	3.82
	5	0.60	8.17	0.65	3.19
	10	0.61	6.28	0.69	2.64
	20	0.63	4.54	0.61	1.75
$NC_{70}BA$	0	0.83	10.73	0.66	5.88
	5	0.84	8.93	0.67	5.06
	10	0.84	8.69	0.69	5.01
	20	0.85	8.25	0.70	4.89

3. Conclusions

We synthesized a new dihydronaphthyl-based [70]fullerene bisadduct derivative ($NC_{70}BA$), which was explored as an acceptor in P3HT-based PSCs. This material has improved absorption and high-lying LUMO energy level, leading to a high PCE (5.95%) for P3HT-based solar cells with this material as acceptor. Moreover, the $NC_{70}BA$ shows an amorphous nature upon heating treatment, so the PSCs fabricated by P3HT:$NC_{70}BA$ have high thermal stability. It was observed that the PCE of P3HT:$NC_{70}BA$-based devices only slightly decreased from 5.88% to 4.89% after 20 h heating at 150 °C. These results indicate that $NC_{70}BA$ is a promising acceptor material for practical use in PSCs.

4. Experimental Section

Materials: All chemicals were purchased from commercial sources and used without further purificaton; the solvents were purified and freshly distilled prior to use according to literature procedures.

Measurements: ^{1}H NMR and ^{13}C NMR spectra were measured on Bruker DMX-400 and Bruker DMX-600 spectrometers. Chemical shifts of NMR are reported in ppm relative to the singlet of $CDCl_3$ at 7.26 ppm for ^{1}H NMR spectroscopy and 77.6 ppm for ^{13}C NMR spectroscopy. Absorption spectra were taken on a Hitachi U-3010 UV–vis spectrophotometer. Electrochemical cyclic voltammetry was conducted on a Zahner IM6e Electrochemical Workstation. During measurement, a Pt disk was used as the working electrode, Pt wire as the counter electrode, and Ag/Ag^+ electrode (0.01 M $AgNO_3$, 0.09 M Bu_4NPF_6 in acetonitrile) as the reference electrode were used in a mixed solution of *o*-dichlorobenzene:acetonitrile (5:1 v/v) with 0.1 M tetrabutylammonium hexafluorophosphate (NBu_4PF_6) at 100 mV s^{-1}. The differential scanning calorimetry (DSC) analysis of fullerene derivatives was performed under a nitrogen atmosphere on a TA Instruments Q-100 at heating rates of 10 °C min^{-1}. Thermogravimetric analysis (TGA) was recorded on TA Q-50 under nitrogen atmosphere at a heating rate of 20 °C min^{-1}. The optical microscopy images were obtained using an Olympus Fluoview Fv1000. High performance liquid chromatography (HPLC) analysis was performed on LC908-C60 (Jai Co., Ltd.) with a Cosmosil Buckyprep column (Φ 20 mm × 250 mm, Nacalai USA) using toluene as eluent.

Synthesis of Sultine: Sodium hydroxymethanesulfinate (rongalite, 402.8 mg, 3.4136 mmol) and tetrabutylammonium bromide (TBAB, 82.5 mg, 0.2561 mmol) were added to a solution of 1,2-bis(bromomethyl)-benzene (225.3 mg, 0.8534 mmol) in DMF (15 mL). The mixture was stirred at 0 °C under an argon atmosphere for 4 h, then water was added and the mixture extracted with CH_2Cl_2. The organic extracts were dried using $NaSO_4$, and the solvent was evaporated at 25 °C. The raw product was subjected to the next reaction without further purification. ^{1}H NMR (400 MHz, $CDCl_3$): δ(ppm) 7.19–7.42 (m, 4H), 5.31 (d, 1H), 4.97 (d, 1H), 4.42 (d, 1H), 3.55 (d, 1H).

Synthesis of $NC_{70}BA$: The sultine (152.1 mg, 0.9 mmol) was added to a solution of C_{70} (252.0 mg, 0.3 mmol) in toluene (250 mL). The mixture was heated to 80 °C under an argon atmosphere for 15 h. After cooling down, water was added and the mixture was extracted with toluene. The organic extracts were dried by using $NaSO_4$, and concentrated under reduced pressure. The raw product was first purified by a silica gel column using toluene as eluent. Further purification by preparative HPLC equipped with a Buckyprep column using toluene as eluent. Yield: 64%. ^{1}H NMR (400 MHz, $CDCl_3$): δ(ppm) 6.98–7.60(m, 8H), 3.66–4.18 (m, 8H). ^{13}C NMR (200 MHz, $CDCl_3$): δ(ppm) 151.00, 150.61, 150.32, 149.96, 148.99, 145.08, 144.50, 143.59, 142.37, 141.93, 141.47, 139.39, 138.71, 138.61, 138.07, 137.96, 135.32, 132.97, 132.51, 129.87, 129.06, 128.68, 128.62, 128.47, 126.13, 78.06, 77.85, 77.64, 60.81, 60.51, 60.08, 59.90, 59.17, 59.05, 58.92, 57.45, 46.02, 45.48, 44.75, 42.77, 41.82. MALDI-TOF MS: calcd. 1048.13; found 1048.67.

Fabrication and Characterization of PSCs: A conventional PSC structure based on ITO/PEDOT:PSS/BHJ/Ca/Al was used. The ITO glass was cleaned by sequential ultrasonic treatment in detergent, deionized water, acetone, and isopropanol, and then treated in an ultraviolet–ozone chamber (Ultraviolet Ozone Cleaner, Jelight Company, USA) for 20 min. Then PEDOT:PSS (poly (3,4-ethylene dioxythiophene):poly(styrene sulfonate)) (Baytron PVPAI 4083, Germany) was filtered through a 0.45 μm filter and spin coated at 4000 rpm for 60 s on the ITO electrode. Subsequently, the PEDOT: PSS film was baked at 150 °C for 20 min in the air. The blend solution of P3HT and different fullerene derivative acceptors in dichlorobenzene (DCB) (total concentration 34 mg mL^{-1}, weight ratio of P3HT:PCBM of 1:1, P3HT:NC_{60}BA of 1:1, P3HT:NC_{70}BA of 1:1.2, and P3HT:PC_{70}BM of 1:1.2) was then spin-coated on top of the PEDOT:PSS layer. The blend films were then put into glass Petri dishes while still wet to undergo solvent annealing. The thickness of the photoactive layer was estimated using a surface profiler in the range 180–220 nm. The device was annealed at 120 °C for 10 min. The thermal stabilities of the P3HT:PCBM- and P3HT:NC_{70} BA-based devices were assessed by subjected them to sustained heating at 150 °C for different times. A bilayer cathode consisted of Ca (20 nm) capped with Al (100 nm) was thermally evaporated under a shadow mask under a base pressure of ca. 10^{-4} Pa. The device active area of the PSC is ca. 4 mm^2. The *J–V* measurement of the devices was conducted on a computer-controlled Keithley 236 Source Measure Unit. Device characterization was done in a glovebox under simulated AM1.5G irradiation (100 mW cm^{-2}) using a xenon lamp-based solar simulator (from Newport Co., Ltd.). The EQE measurements of the PSCs were performed using a Stanford Research Systems model SR830 DSP lock-in amplifier coupled with WDG3 monochromator and 500W xenon lamp. The light intensity at each wavelength was calibrated with a standard single-crystal Si photovoltaic cell.

Supporting Information

Supporting Information is available from the Wiley Online Library or from the author.

Acknowledgements

This work was supported by the Ministry of Science and Technology 973 (No. 2011CB302100), the National Basic Research Program (Nos. 2012CB932900 and 2011CB933700), and the NSFC (Nos. 91027018, 20903107, 21121063, 21004019 and 51173040).

Received: November 16, 2011
Revised: January 10, 2012
Published online: February 27, 2012

[1] a) S. Gunes, H. Neugebauer, N. S. Sariciftci, *Chem. Rev.* **2007**, *107*, 1324; b) B. C. Thompson, J. M. J. Frechet, *Angew. Chem. Int. Ed.* **2008**, *47*, 58; c) L. M. Chen, Z. R. Hong, G. Li, Y. Yang, *Adv. Mater.* **2009**, *21*, 1434; d) G. Dennler, M. C. Scharber, C. J. Brabec, *Adv. Mater.* **2009**, *21*, 1323.

[2] G. Yu, J. Gao, J. C. Hummelen, F. Wudl, A. J. Heeger, *Science.* **1995**, *270*, 1789.

[3] a) G. Li, V. Shrotriya, J. Huang, Y. Yao, T. Moriarty, K. Emery, Y. Yang, *Nat. Mater.* **2005**, *4*, 864; b) W. Ma, C. Yang, X. Gong, K. Lee, A. J. Heeger, *Adv. Funct. Mater.* **2005**, *15*, 1617; c) Y. Kim, S. Cook, S. M. Tuladhar, S. A. Choulis, J. Nelson, J. R. Durrant, D. D. C. Bradley, M. Giles, I. McCulloch, C.-S. Ha, M. Ree, *Nat. Mater.* **2006**, *5*, 197.

[4] a) J. Chen, Y. Cao, *Acc. Chem. Res.* **2009**, *42*, 1709; b) Y.-J. Cheng, S.-H. Yang, C.-S. Hsu, *Chem. Rev.* **2009**, *109*, 5868.

[5] Y. He, Y. Li, *Phys. Chem. Chem. Phys.* **2011**, *13*, 1970.

[6] a) Y. Liang, Z. Xu, J. Xia, S.-T. Tsai, Y. Wu, G. Li, C. Ray, L. Yu, *Adv. Mater.* **2010**, *22*, E135; b) Z. He, C. Zhong, X. Huang, W.-Y. Wong, H. Wu, L. Chen, S. Su, Y. Cao, *Adv. Mater.* **2011**, *23*, 4636; c) H. Zhou, L. Yang, A. C. Stuart, S. C. Price, S. Liu, W. You, *Angew. Chem. Int. Ed.* **2011**, *50*, 2995; d) C. Piliego, T. W. Holcombe, J. D. Douglas, C. H. Woo, P. M. Beaujuge, J. M. J. Fréchet, *J. Am. Chem. Soc.* **2010**, *132*, 7595; e) C. M. Amb, S. Chen, K. R. Graham, J. Subbiah, C. E. Small, F. So, J. R. Reynolds, *J. Am. Chem. Soc.* **2011**, *133*, 10062; f) T.-Y. Chu, J. Lu, S. Beaupré, Y. Zhang, J.-R. m. Pouliot, S. Wakim, J. Zhou, M. Leclerc, Z. Li, J. Ding, Y. Tao, *J. Am. Chem. Soc.* **2011**, *133*, 4250; g) S. C. Price, A. C. Stuart, L. Yang, H. Zhou, W. You, *J. Am. Chem. Soc.* **2011**, *133*, 4625; h) H. J. Son, W. Wang, T. Xu, Y. Liang, Y. Wu, G. Li, L. Yu, *J. Am. Chem. Soc.* **2011**, *133*, 1885; i) H.-Y. Chen, J. H. Hou, S. Q. Zhang, Y. Y. Liang, G. W. Yang, Y. Yang, L. P. Yu, Y. Wu, G. Li, *Nat. Photonics* **2009**, *3*, 649; j) L. J. Huo, S. Q. Zhang, X. Guo, F. Xu, Y. F. Li, J. H. Hou, *Angew. Chem. Int. Ed.* **2011**, *50*, 9697.

[7] a) J. A. Mikroyannidis, A. N. Kabanakis, S. S. Sharma, G. D. Sharma, *Adv. Funct. Mater.* **2011**, *21*, 746; b) J. A. Mikroyannidis, D. V. Tsagkournos, S. S. Sharma, G. D. Sharma, *J. Phys. Chem. C* **2011**, *115*, 7806.

[8] a) G. Zhao, Y. He, Z. Xu, J. Hou, M. Zhang, J. Min, H.-Y. Chen, M. Ye, Z. Hong, Y. Yang, Y. Li, *Adv. Funct. Mater.* **2010**, *20*, 1480; b) H. Zhao, X. Guo, H. Tian, C. Li, Z. Xie, Y. Geng, F. Wang, *J. Mater. Chem.* **2010**, *20*, 3092; c) K. Matsumoto, K. Hashimoto, M. Kamo, Y. Uetani, S. Hayase, M. Kawatsura, T. Itoh, *J. Mater. Chem.* **2010**, *20*, 9226; d) H. J. Bolink, E. Coronado, A. Forment-Aliaga, M. Lenes, A. La Rosa, S. Filippone, N. Martin, *J. Mater. Chem.* **2011**, *21*, 1382; e) A. Tamayo, T. Kent, M. Tantitiwat, M. A. Dante, J. Rogers, T.-Q. Nguyen, *Energy Environ. Sci.* **2009**, *2*, 1180.

[9] a) F. B. Kooistra, J. Knol, F. Kastenberg, L. M. Popescu, W. J. H. Verhees, J. M. Kroon, J. C. Hummelen, *Org. Lett.* **2007**, *9*, 551; b) M. Murata, Y. Morinaka, Y. Murata, O. Yoshikawa, T. Sagawa, S. Yoshikawa, *Chem. Commun.* **2011**, *47*, 7335; c) A. Varotto, N. D. Treat, J. Jo, C. G. Shuttle, N. A. Batara, F. G. Brunetti, J. H. Seo, M. L. Chabinyc, C. J. Hawker, A. J. Heeger, F. Wudl, *Angew. Chem. Int. Ed.* **2011**, *50*, 5166; d) C.-P. Chen, Y.-W. Lin, J.-C. Horng, S.-C. Chuang, *Adv. Energy Mater.* **2011**, *1*, 776.

[10] C. J. Brabec, A. Cravino, D. Meissner, N. S. Sariciftci, T. Fromherz, M. T. Rispens, L. Sanchez, J. C. Hummelen, *Adv. Funct. Mater.* **2001**, *11*, 374.

[11] a) M. Lenes, G. Wetzelaer, F. B. Kooistra, S. C. Veenstra, J. C. Hummelen, P. W. M. Blom, *Adv. Mater.* **2008**, *20*, 2116; b) M. Lenes, S. W. Shelton, A. B. Sieval, D. F. Kronholm, J. C. Hummelen, P. W. M. Blom, *Adv. Funct. Mater.* **2009**, *19*, 3002.

[12] a) R. B. Ross, C. M. Cardona, D. M. Guldi, S. G. Sankaranarayanan, M. O. Reese, N. Kopidakis, J. Peet, B. Walker, G. C. Bazan, E. Van Keuren, B. C. Holloway, M. Drees, *Nat. Mater.* **2009**, *8*, 208; b) R. B. Ross, C. M. Cardona, F. B. Swain, D. M. Guldi, S. G. Sankaranarayanan, E. Van Keuren, B. C. Holloway, M. Drees, *Adv. Funct. Mater.* **2009**, *19*, 2332.

[13] a) Y. J. He, G. J. Zhao, B. Peng, Y. F. Li, *Adv. Funct. Mater.* **2010**, *20*, 3383; b) Y. He, B. Peng, G. Zhao, Y. Zou, Y. Li, *J. Phys. Chem. C* **2011**, *115*, 4340; c) C.-Z. Li, S.-C. Chien, H.-L. Yip, C.-C. Chueh, F.-C. Chen, Y. Matsuo, E. Nakamura, A. K. Y. Jen, *Chem. Commun.* **2011**, *47*, 10082; d) Y.-J. Cheng, M.-H. Liao, C.-Y. Chang, W.-S. Kao, C.-E. Wu, C.-S. Hsu, *Chem. Mater.* **2011**, *23*, 4056; e) E. Voroshazi, K. Vasseur, T. Aernouts, P. Heremans, A. Baumann, C. Deibel, X. Xue, A. J. Herring, A. J. Athans, T. A. Lada, H. Richter, B. P. Rand, *J. Mater. Chem.* **2011**, *21*, 17345; f) K.-H. Kim, H. Kang, S. Y. Nam, J. Jung, P. S. Kim, C.-H. Cho, C. Lee, S. C. Yoon, B. J. Kim, *Chem. Mater.* **2011**, *23*, 5090.

[14] Y. J. He, H. Y. Chen, J. H. Hou, Y. F. Li, *J. Am. Chem. Soc.* **2010**, *132*, 1377.

[15] G. J. Zhao, Y. J. He, Y. F. Li, *Adv. Mater.* **2010**, *22*, 4355.

[16] X. Y. Meng, W. Q. Zhang, Z. A. Tan, C. Du, C. H. Li, Z. S. Bo, Y. F. Li, X. L. Yang, M. M. Zhen, F. Jiang, J. P. Zheng, T. S. Wang, L. Jiang, C. Y. Shu, C. R. Wang, *Chem. Commun.* **2012**, *48*, 425.

[17] M. M. Wienk, J. M. Kroon, W. J. H. Verhees, J. Knol, J. C. Hummelen, P. A. van Hal, R. A. J. Janssen, *Angew. Chem. Int. Ed.* **2003**, *42*, 3371.

[18] a) J. L. Segura, N. Martín, *Chem. Rev.* **1999**, *99*, 3199; b) S. A. Backer, K. Sivula, D. F. Kavulak, J. M. J. Fréchet, *Chem. Mater.* **2007**, *19*, 2927.

[19] M. D. Hoey, D. C. Dittmer, *J. Org. Chem.* **1991**, *56*, 1947.

[20] Q. Sun, H. Wang, C. Yang, Y. Li, *J. Mater. Chem.* **2003**, *13*, 800.

[21] Y. Zhang, H. L. Yip, O. Acton, S. K. Hau, F. Huang, A. K. Y. Jen, *Chem. Mater.* **2009**, *21*, 2598.